The inner magnetosphere of Saturn: Cassini RPWS cold plasma results from the first encounter.

J.-E. Wahlund, R. Boström, G. Gustafsson, D.A. Gurnett, W.S. Kurth, T. Averkamp, G.B. Hospodarsky, A.M. Persoon, P. Canu, A. Pedersen, et al.

The inner magnetosphere of Saturn: Cassini RPWS cold plasma results from the first encounter

J.-E. Wahlund,[1] R. Boström,[1] G. Gustafsson,[1] D. A. Gurnett,[2] W. S. Kurth,[2] T. Averkamp,[2] G. B. Hospodarsky,[2] A. M. Persoon,[2] P. Canu,[3] A. Pedersen,[4] M. D. Desch,[5] A. I. Eriksson,[1] R. Gill,[1] M. W. Morooka,[1] and M. André[1]

Received 14 February 2005; revised 28 July 2005; accepted 9 August 2005; published 2 September 2005.

[1] We present new results from the inner magnetosphere of Saturn obtained by the Radio and Plasma Wave Science (RPWS) investigation onboard Cassini around the period of the Saturn orbit injection (July 1, 2004). Plasma wave electric field emissions, voltage sweeps by the Langmuir probe (LP) and radio sounder data were used to infer the cold plasma (<100 eV) characteristics within 20 R_S of Saturn. A dense (<150 cm^{-3}) and cold (<7 eV) plasma torus was found just outside the visible F-ring. This torus of partly dusty plasma does not perfectly co-rotate with Saturn, which suggests the cold plasma is electro-dynamically coupled to the charged ring-dust particles. The spacecraft potential was a few volts negative above the E- and G-rings, indicating the dust-particles were likewise negatively charged. The cold ion characteristics changed near the magnetically conjugate position of Dione, indicating release of volatile material from this icy moon. **Citation:** Wahlund, J.-E., et al. (2005), The inner magnetosphere of Saturn: Cassini RPWS cold plasma results from the first encounter, *Geophys. Res. Lett.*, *32*, L20S09, doi:10.1029/2005GL022699.

1. Introduction

[2] Three spacecraft have earlier made observations of the inner magnetosphere of Saturn. Pioneer 11 provided information of energetic ions (100 eV–8 keV) at distances 4–16 R_S from Saturn and within 1 R_S from the equatorial plane [*Frank et al.*, 1980]. These data pointed to a dense (>1 cm^{-3}) and rigidly co-rotating magnetosphere out to a distance of ~10 R_S, but slightly less so beyond this distance. Maximum ion number densities near the icy moons of Tethys and Dione were close to 50 cm^{-3}, and indicated that the orbits of these moons where surrounded by plasma torii around Saturn. The Voyager 1 and 2 trajectories were steeper in latitude past Saturn, but the PLS instrument (10 eV–6 keV) nevertheless confirmed the largely co-rotating behaviour of the magnetosphere beyond 4 R_S [e.g., *Bridge et al.*, 1982; *Sittler et al.*, 1983; *Richardson*, 1986]. Co-rotation was also here systematically slower by up to 50% outside the 6–9 R_S range. Only Voyager-2 showed a strict co-rotation within 6 R_S, while Voyager-1 data revealed a sharp drop from co-rotation within 5 R_S. The maximum plasma density near the equator of the L-shell of Dione was 20–25 cm^{-3} and consisted mostly of ions with a mass number around 16 amu. The spectral peak was broad enough to include N^+, O^+, OH^+ or H_2O^+.

[3] The Cassini spacecraft reached on its orbit injection (SOI) trajectory much deeper into the magnetosphere of Saturn and crossed the equatorial plane twice just outside the F-ring at ~2.5 R_S. The closest approach was only 1.3 R_S from the centre of Saturn above the visible rings. The plasma observations reported here provide new data at energies below 100 eV, an energy range not covered to the same extent on previous missions. The treatment is restricted to the results from the first encounter.

2. Observations

2.1. Measurement Principles

[4] For a description of the RPWS instrument see *Gurnett et al.* [2004]. The electron number density (n_e) can be estimated with numerous methods with several instruments on board Cassini. The RPWS investigation employs at least three different methods for this purpose. One method makes use of the upper hybrid emission line which peak in electric spectra at the frequency $f_{UH} \approx \sqrt{f_{ge}^2 + f_{pe}^2}$, where f_{ge} is the electron gyro-frequency and f_{pe} is the electron plasma frequency. Knowing the magnetic field strength gives n_e. Some other emission lines and propagation cut-off frequencies can likewise be used to estimate n_e as described by, e.g., *Gurnett et al.* [2005]. The second method employs an active sounder connected to the electric antenna, which triggers with an emitter, the characteristic resonances of the surrounding plasma from which f_{pe}, and hence n_e, is derived. A third method makes use of the fact that the Langmuir probe sensor samples the total electron number density surrounding the spacecraft. This method, described in more detail below, in addition gives estimates of several other cold plasma parameters of importance for characterizing the properties of the inner magnetosphere of Saturn.

2.2. Electron Density and Temperature

[5] The electron parameter results of a two-electron component Orbit Motion Limited (OML) theory [*Mott-Smith and Langmuir*, 1926] fit to the LP potential sweeps (±32 V) versus distance from Saturn are shown in Figure 1. The data are from the 2 days around SOI. The overall symmetry between the inbound (red) and outbound (black) parameter values is striking. The estimated electron number densities

[1]Swedish Institute of Space Physics, Uppsala, Sweden.
[2]Department of Physics and Astronomy, University of Iowa, Iowa City, Iowa, USA.
[3]Centre d'Etude des Environnements Terrestre et Planétaires, Velizy-Villacoublay, France.
[4]Department of Physics, Oslo University, Oslo, Norway.
[5]NASA Goddard Space Flight Center, Greenbelt, Maryland, USA.

0094-8276/05/2005GL022699

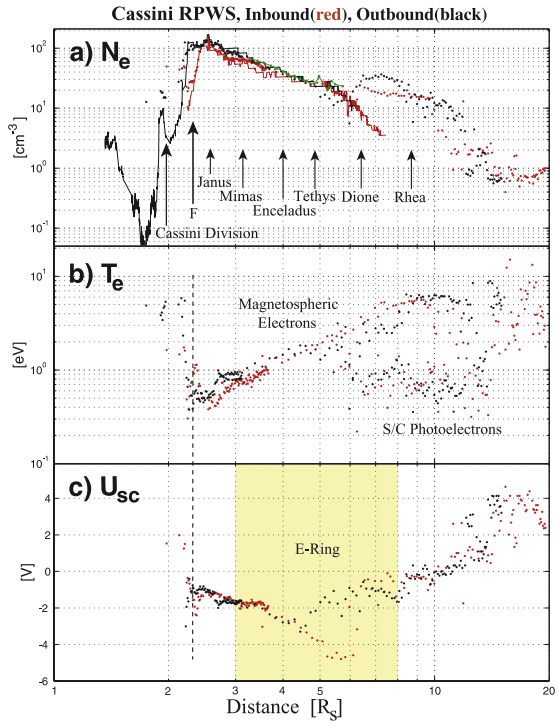

Figure 1. The cold electron plasma properties in the inner magnetosphere of Saturn as estimated by RPWS. In the panels are the electron number density (n_e, panel a), the electron temperature (T_e, panel b) and the spacecraft potential (U_{SC}, panel c) for June 30 and July 1, 2004. The inbound (red) and outbound (black) potential sweep data (dots) is superposed on the upper hybrid emission derived densities (red and black lines) and sounder data (green, outbound only).

(n_e) from upper hybrid and other plasma emissions (red/black lines), as well as from the Sounder (green, outbound only), are superposed on the LP sweep results (red/black dots, panel a). This comparison reveals that the three experimental methods give consistent values for the electron number density except in the distance interval 6–7 R_S. It is possible that spacecraft photoelectrons in the region 6–14 R_S partly contribute to the total sampled electron current by the LP, which is further supported by the identification of two cold electron populations with different temperatures (panel b) in this region. One has a $T_e \approx 0.7$ eV, consistent with a photoelectron population, and the other has an increasing trend from a distance of ~2.3 R_S of $T_e \approx 0.5$ eV up to $T_e \approx 6$ eV at 10 R_S. The latter we believe is the magnetospheric core electron population.

[6] Figures 2 and 3 give two examples of LP current-voltage characteristics in both linear and logarithmic scale together with OML theoretical fits. The data in Figure 2 is taken near the peak density at 2.5 R_S and show one electron population, while the data in Figure 3 is taken from the region with two different T_e values and show the signature of two different electron populations with a break in slopes around +15 V. The excellent quality of the model fits to the sweep data allow for errors of at most 40%. Two other error sources could affect the data quality. If the LP is situated in the wake of the spacecraft as compared to the plasma flow direction, the density may become underestimated. This happened for a short duration on the outbound near 3 R_S, but gave only a very small signature change of at most 20% in the estimated number density. The other error source appears when densities fall below 30 cm^{-3} and the Debye length becomes larger than the distance between the LP sensor and the spacecraft (1.5 m), and spacecraft photoelectrons may become a problem. The amount of contamination from spacecraft photoelectrons depends on both electrical potential of the spacecraft and its attitude versus the Sun. This contribution is often hard to predict.

[7] Ring particles should have potentials close to the spacecraft potential (U_{SC}) on conjugate magnetic field lines, since a similar current balance occurs on their surfaces with the surrounding plasma. The relative amount of emitted photoelectrons varies somewhat depending on surface properties, and may result in different charge states. We note that the E-ring particles therefore should become negatively charged (up to −5 V, Figure 1c), which is supported by

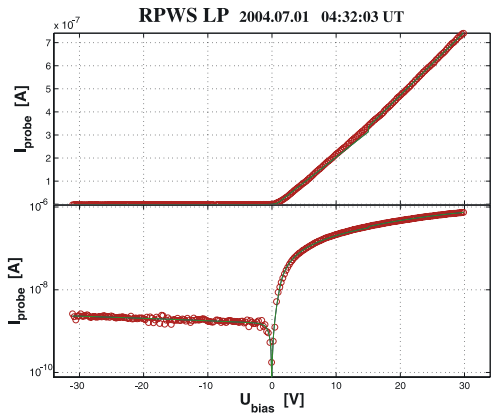

Figure 2. The sweep voltage-current characteristic (red circles) from a period near the maximum density of the ring-dust torus. Both the linear (upper panel) as well as the logarithmic (lower panel) versions of the characteristic is shown. The best OML fit (green line) is superposed on the data.

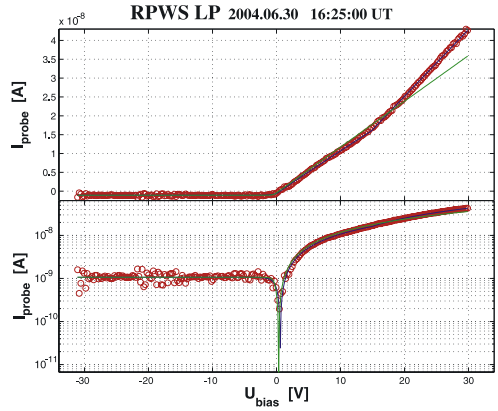

Figure 3. Same as in Figure 2, but for a time where two electron components could be detected. See the break in slope near +15 V. A two-electron component OML fit result (blue line) has been added.

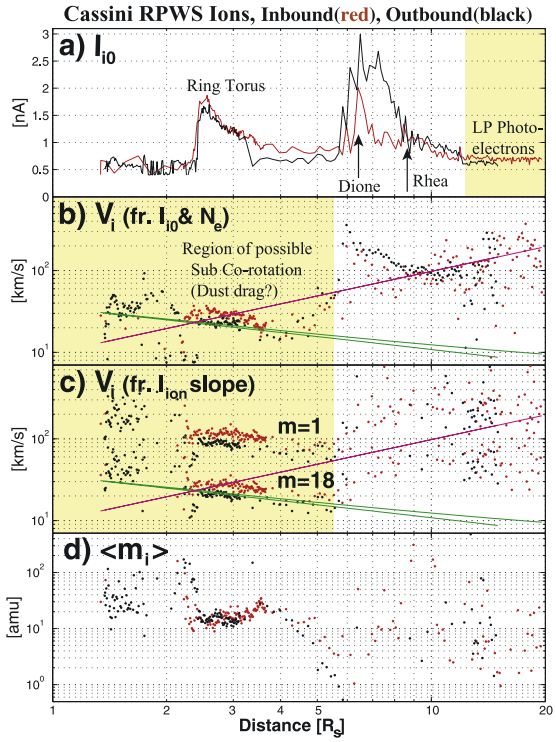

Figure 4. Derived ion parameters from the negative potential characteristic of the LP sweeps during the two days around SOI. The displayed parameters are total probe current (panel a), ion ram speed derived from the dc current (panel b), ion ram speeds from the ion current slope assuming proton and water group ions (panel c), and the averaged ion mass (panel d). Superposed on the ion ram speed are the magnetospheric co-rotation speed (magenta) and the spacecraft speed (green). The regions of photoelectron probe current domination is shaded yellow in panel a. The region of sub co-rotation is shaded yellow in panels b and c.

the dust counter instrument (CDA, R. Srama, private communication, 2005).

2.3. Observations of Ions

[8] The LP sweep data can also, in some circumstances, be used to obtain values for the average ion mass, ion ram velocity, ion density, ion temperature, and solar UV intensity [e.g., *Fahleson et al.*, 1974]. The current to the probe for negative U_{bias} is given by $I = I_{i0}\,(1 - U_{bias}/T_{i,eff}) + I_{ph}$, where the effective ion energy ($T_{i,eff}$) is the sum of the thermal random ion temperature (T_i) and the ram ion directed flow energy ($m_i v_i^2/2e$ [eV]).

[9] The total dc current ($I_{i0} + I_{ph}$) is displayed in Figure 4a. The electrical current to the probe for a fixed negative potential is normally dominated by the photoelectrons emitted from the LP (I_{ph}) under the action of solar UV light and gives a nearly constant contribution (~0.7 nA, shaded yellow in panel a). The additional contribution of magnetospheric ions gives an enhancement above this nearly constant background of photoelectron current. Clear signatures of changes in the ion characteristics occur at the magnetically conjugate distance of the icy moon Dione (at 6.3 R_S) and perhaps at Rhea (8.7 R_S). Clear signatures occur also for the ring-dust plasma torus. The electrical current signatures (1.5–2 nA) here are somewhat less than the Dione current signatures (2–3 nA), while the electron number densities (see Figure 1) differ by almost an order of magnitude. Since $I_{i0} \propto n_i v_i$ and $n_i\sqrt{(T_i/m_i)}$, this can be accounted for if the thermal energy (T_i) is larger by two orders of magnitude in the Dione related plasma (or similar variations in v_i and m_i). One possible error source here is secondary electrons resulting from impacts on the probe surface of a few hundred eV particles, giving in turn an excess current for negative bias potential. However, the absence of substantial positive charging of the spacecraft and the simultaneous increase of the electron current gives us indirect proof that this process was not of importance.

[10] The dc current (I_{i0}) is proportional to the ram flux of ions ($n_i v_i$). By using the condition that the plasma must be electrically neutral, $n_e = n_i$, it is possible to estimate the ion ram speed (v_i), which is displayed in Figure 4b. The LP data are consistent with a co-rotating magnetosphere within a 50% error margin outside 5 R_S. The departure from co-rotation near the distance of Dione is consistent with a warm $T_i \sim 2$–3 keV water group plasma. An intriguing result is that in the range 2.5–5 R_S in the ring-dust plasma torus the estimated ion ram speed is significantly less compared to the expected co-rotation speed (magenta). Instead the ion ram speed follows the spacecraft speed (green) to both value and trend with distance from Saturn. The data are more accurate for slower speeds and larger densities.

[11] An independent estimate of the ion ram speed can be obtained from the slope of the ion current-bias voltage characteristic, i.e. from $T_{i,eff} \propto m_i v_i^2/2e$, by assuming values of the averaged ion mass m_i. In Figure 4c the resulting ion ram speed values are shown for water group ions (18 amu) and protons (1 amu). The $T_{i,eff}$ becomes uncertain and underestimated for large energies (>100 eV, small slope). This analysis confirms that the ion ram speed follows the spacecraft speed rather than the co-rotation speed within 5 R_S.

[12] The average ion mass (m_i), obtained by using the ion ram speed estimate in panel b and $T_{i,eff}$, is about 15–20 amu in the ring-dust torus and consistent with water ion products. Lower mass ions like H^+ become more abundant outward from Saturn and m_i stayed around 10 amu in the outer magnetosphere. Errors may be large in the outer magnetosphere because of the small ion current contribution to the probe current as compared to the dominant photoelectron current. Heavier ions were detected above the ring plane, which is consistent with INMS data indicating a domination of O_2^+ ions there [*Waite et al.*, 2005].

3. Discussion and Conclusions

[13] The RPWS cold plasma results identify four magnetospheric regions characterized by different ion composition and dynamics, as well as different plasma densities and temperatures, which reflect different source, loss and transport mechanisms. The inner magnetosphere showed a large degree of symmetry between the inbound and outbound passes, except near the F-ring. The plasma above the visible rings is tenuous (0.01–20 cm^{-3}) and a few eV hot. The low density can be due to absorption of the magnetically mirroring plasma particles by the ring particles themselves

in the ring plane [see, e.g., *Van Allen et al.*, 1980]. The increased n_e on conjugate magnetic field lines to the Cassini division, which contains less ring particles, supports this view. The source of this plasma is likely to be meteorite impacts on ring particles, photo-ionization of the neutral ring atmosphere, the ionosphere of Saturn and possibly cross-magnetic field diffusion from the ring-dust torus. The spacecraft was in shadow by the rings between 1.7 R_S and the A-ring edge during the outbound, which limits photo-ionization there. The ring-dust plasma torus (or "ring ionosphere") inferred from the Voyager measurements [*Gan-Barush et al.*, 1994] was found to be dense (10–150 cm^{-3}) and consist of water group ions (15–20 amu). The electron temperature increase from 0.5 eV near the ring plane crossing to 6 eV near 10 R_S (in plasma sheath) is in qualitative agreement with recent model results where the ionization of the H_2O atmosphere of the rings give rise to the plasma torus [*Ip*, 2000] and earlier Voyager results [*Sittler et al.*, 1983] as well as recent Cassini results [*Young et al.*, 2005]. The plasma sheath had densities between 2–20 cm^{-3}. The discrepancy between the f_{UH} derived electron number density and the LP in the 6–7 R_S is still an open issue, but the LP was here indeed contaminated by photo-electrons from the spacecraft. The outer magnetosphere beyond 14 R_S was found hot (T_e > few eV) and tenuous ($n_e \sim 0.1–0.5$ cm^{-3}) and to consist of lighter ions (<10 amu). However, the errors may be large in this tenuous plasma.

[14] The magnetosphere was found to be co-rotating within an error margin of 50%, except inside ~5 R_S where the cold ion population clearly was rotating with a speed significantly below the co-rotation speed. Within ~4 R_S the ion speed must have been slower than the spacecraft speed. This result is in contrast to recent CAPS results outside ~4 R_S [*Sittler et al.*, 2005] and the Voyager-2 PLS results outside 4.5 R_S, which showed strict co-rotation. However, the Voyager-1 PLS measurements did indeed indicate a drop from co-rotation by 20–30 km/s inside 5 R_S [*Saur et al.*, 2004]. The disagreement between the RPWS LP and CAPS results need further investigation.

[15] There are several possible reasons for the plasma within 6 R_S to slow down. *Saur et al.* [2004] presents a model where an increase in the magnetospheric conductance due to collisions can cause the azimuthal velocity to drop. Moreover, the dust rings and icy moons are surrounded by a dense neutral cloud [*Ip*, 2000], which after photo-ionization could cause a heavy mass load in the inner magnetospheric plasma.

[16] In the sub co-rotating region observed by RPWS LP the spacecraft potential was a few Volt negative, which suggests that the E-ring/G-ring dust particles also should be negatively charged. We therefore suggest sub co-rotation can be due to a collective electric coupling between charged dust particles and the surrounding plasma. The ring particles are influenced by the slower Keplerian gravitational motion, while the plasma is influenced by the induced co-rotation electric field and resulting $\mathbf{E} \times \mathbf{B}$ motion of the magnetosphere. In order for the charged dust to have a significant effect on the co-rotating plasma the gravitational force associated with the dust need be of the same order of magnitude as the force of the co-rotating ions within the coupled dust-MHD equations, i.e., $q_i n_i (2\pi/\tau_{rot}) rB \sim n_d m_d GM_S/r^2$. A 1–5 μm water-dust grain will have a mass of about $4 \cdot 10^{-15}$–$4 \cdot 10^{-12}$ kg, which gives a requirement of the number of dust particles of 0.2–300 dust/m^3 for comparable momentum transfer. The CDA instrument saturates at ~1 dust/m^3 near the ring plane in the E-ring (R. Srama, private communication, 2005). It is therefore possible that charged dust could have an effect on the motion of the plasma. A rather complex dust-plasma interaction should also occur near the F-ring, where an asymmetry in the plasma characteristics was detected (Figure 1a).

[17] **Acknowledgments.** The Swedish National Space Board (SNSB) supports the RPWS LP instrument on board Cassini. We thank F. Crary for useful discussions.

References

Bridge, H. S., et al. (1982), Plasma observations near Saturn: Initial results from Voyager 2, *Science*, *215*, 563.

Fahleson, U., C.-G. Fälthammar, and A. Pedersen (1974), Ionospheric temperature and density measurements by means of spherical double probes, *Planet. Space Sci.*, *22*, 41.

Frank, L. A., B. G. Bureck, K. L. Ackerson, J. H. Wolfe, and J. D. Mihalov (1980), Plasma in Saturn's magnetosphere, *J. Geophys. Res.*, *85*, 5695.

Gan-Barush, Z., A. Eviatar, J. D. Richardson, and R. L. McNutt Jr. (1994), Plasma observations near the ring plane of Saturn, *J. Geophys. Res.*, *99*, 11,063.

Gurnett, D. A., et al. (2004), The Radio and Plasma Wave Science Investigation, *Space Sci. Rev.*, *114*, 395.

Gurnett, D. A., et al. (2005), Cassini radio and plasma wave observations near Saturn, *Science*, *307*, 1255.

Ip, W.-H. (2000), Thermal plasma composition in Saturn's magnetosphere, *Planet. Space Sci.*, *48*, 775.

Mott-Smith, H. M., and I. Langmuir (1926), The theory of collectors in gaseous discharges, *Phys. Rev.*, *28*, 727.

Richardson, J. D. (1986), Thermal ions at Saturn: Plasma parameters and implications, *J. Geophys. Res.*, *91*, 1381.

Saur, J., B. H. Mauk, A. Kaßner, and F. M. Neubauer (2004), A model for the azimuthal plasma velocity in Saturn's magnetosphere, *J. Geophys. Res.*, *109*, A05217, doi:10.1029/2003JA010207.

Sittler, E. C., Jr., K. W. Ogilvie, and J. D. Scudder (1983), Survey of low energy electrons in Saturn's magnetosphere: Voyager 1 and 2, *J. Geophys. Res.*, *88*, 8847.

Sittler, E. C., Jr., et al. (2005), Preliminary results on Saturn's inner plasmasphere as observed by Cassini: Comparison with Voyager, *Geophys. Res. Lett.*, *32*, L14S07, doi:10.1029/2005GL022653.

Van Allen, J. A., B. A. Randall, and M. F. Thomsen (1980), Sources and sinks of energetic electrons and protons in Saturn's magnetosphere, *J. Geophys. Res.*, *85*, 5679.

Waite, H., et al. (2005), Cassini ion and neutral mass spectrometer measurements of oxygen ions near Saturn's A-ring, *Science*, *307*, 1260.

Young, D. T., et al. (2005), Composition and dynamics of plasma in Saturn's magnetosphere, *Science*, *307*, 1262.

M. André, R. Boström, A. I. Eriksson, R. Gill, G. Gustafsson, M. W. Morooka, and J.-E. Wahlund, Swedish Institute of Space Physics, Uppsala Division, P.O. Box 537, SE-751 21 Uppsala, Sweden. (ma@irfu.se; rb@irfu.se; aie@irfu.se; rg@irfu.se; gg@irfu.se; michiko@irfu.se; jwe@irfu.se)

T. Averkamp, D. A. Gurnett, G. B. Hospodarsky, W. S. Kurth, and A. M. Persoon, Department of Physics and Astronomy, University of Iowa, Iowa City, IA 52242-1479, USA. (wtr@space.physics.uiowa.edu; dag@space.physics.uiowa.edu; gbh@space.physics.uiowa.edu; wsk@space.physics.uiowa.edu; amp@space.physics.uiowa.edu)

P. Canu, Centre d'Etude des Environnements Terrestre et Planétaires, F-78140 Velizy-Villacoublay, France. (patrick.canu@cetp.ipsl.fr)

A. Pedersen, Department of Physics, Oslo University, N-0316 Oslo, Norway. (arne.pedersen@fys.uio.no)

M. D. Desch, NASA Goddard Space Flight Center, Greenbelt, MD 20771, USA. (mdesch@pop600.gsfc.nasa.gov)